Flexible multidimensional modulation formats based on PM-QPSK constellations for elastic optical networks

Zilong He (何子龙)[1,*], Wentao Liu (刘文涛)[1], Bailin Shen (沈百林)[2], Xue Chen (陈 雪)[1], Xiqing Gao (高夕晴)[1], Sheping Shi (施社平)[2], Qi Zhang (张 琦)[2], Dongdong Shang (尚冬冬)[2], Yongning Ji (吉勇宁)[2], and Yingfeng Liu (刘英峰)[2]

[1]*State Key Lab of Information Photonics and Optical Communications, Beijing University of Posts and Telecommunications, Beijing 100876, China*

[2]*ZTE Corporation, Beijing 100191, China*

**Corresponding author: hzl_bupt@163.com*

Received September 5, 2015; accepted February 23, 2016; posted online March 18, 2016

We demonstrate flexible multidimensional modulation formats, polarization multiplexed k-symbol check quadrature phase shift keying (PM-kSC-QPSK), based on PM-QPSK constellations for elastic optical networks. The experimental results show a significant optical signal noise ratio (OSNR) tolerance improvement for PM-2SC-QPSK and PM-4SC-QPSK over PM-QPSK in both back-to-back and 500 km transmission scenarios at the expense of spectral efficiency reduction. This flexible modulation method can be used in elastic optical networks to provide a trade-off between the spectral efficiency and OSNR tolerance.

OCIS codes: 060.1660, 060.2360, 060.4080.
doi: 10.3788/COL201614.040602.

Currently, elastic optical networks[1] and software defined networks[2] have been touted as solutions for enhanced spectral efficiency (SE) and optimized network resource utilization. These architectures require transceivers with a tunable modulation format and symbol rate to support trade-offs among optical reach, bit rate, and SE[3]. There exist several approaches to realize flexibility in both reach and bit rate. In principle, reach can simply be traded against SE and bit rate by employing polarization multiplexed m-ary quadrature amplitude modulation (PM-mQAM) with varying size m of the modulation alphabet[4–7]. However, because available modulation formats, such as PM quadrature phase shift keying (QPSK) and PM-16QAM, have a big difference in terms of SE and achievable transmission distance, the resulting options in terms of deployment are insufficient for flexible systems.

The granularity of this trade-off can be further refined by time domain interleaving of symbols belonging to different sizes m of the modulation alphabet. The resulting modulation formats are referred to as time-domain hybrid QAM[8]. Additionally, rate adaptive forward error correction (FEC) codes can be employed for an extra degree of freedom[9]. In such schemes, the FEC code rate and the size of the modulation alphabet are adjusted to optimally support the desired net bit rate over a requested reach. However, some studies suggest that rate adaptive FEC requires a significant additional hardware effort, thus increasing the transceiver cost[8]. Another option for achieving a finer granularity is the application of alternative modulation formats in four-dimensional (4D) signal space, which have recently received a lot of attention due to their interesting features. For instance, polarization-switched QPSK (PS-QPSK) was identified as the most power-efficient modulation format[10] in four dimensions and can be derived from PM-QPSK by using the Ungerboeck's set-partitioning scheme[11] in four dimensions, where the minimum Euclidean distance between the constellation points is increased by $\sqrt{2} \approx 1.76$ dB after one partition[12,13]. Similarly, another popular 4D format 128-SP-QAM can be derived from PM-16QAM by set partitioning, i.e., a subset of $M = 128$ points out of 256 are chosen from the PM-16QAM constellation by increasing the minimum Euclidean distance[14].

In this Letter, we first present the flexible multidimensional modulation method, PM-kSC-QPSK (SC: symbol check), and then describe the experimental investigations of the back-to-back (B2B) and 500 km transmission performance of PM-2SC-QPSK and PM-4SC-QPSK, with PM-QPSK as the reference at the same symbol rate of 32 Gbaud (i.e., at the bit rates of 96 Gb/s for PM-2SC-QPSK, 112 Gb/s for PM-4SC-QPSK, and 128 Gb/s for PM-QPSK). The results show that PM-2SC-QPSK and PM-4SC-QPSK reduce the optical signal noise ratio (OSNR) required to achieve a bit error rate (BER) of 10^{-3} with 3 and 2 dB, respectively, compared to PM-QPSK in 500 km transmission. This method can be used in elastic optical networks to enable trade-off between SE and OSNR tolerance.

Figure 1 shows the schematic diagram of the flexible multidimensional modulation method based on the PM-QPSK constellations (this method also can be applied on other kind of constellations, such as PM-16QAM). We use the single-parity check (SPC) to correlate k consecutive symbols at the transmitter, shown in Fig. 1(a), and each group of k consecutive symbols are decoded together by using a joint-decision algorithm at the receiver. The signal space is expanded to 2 k-dimensional, since these k-related QPSK symbols can be regarded as a whole.

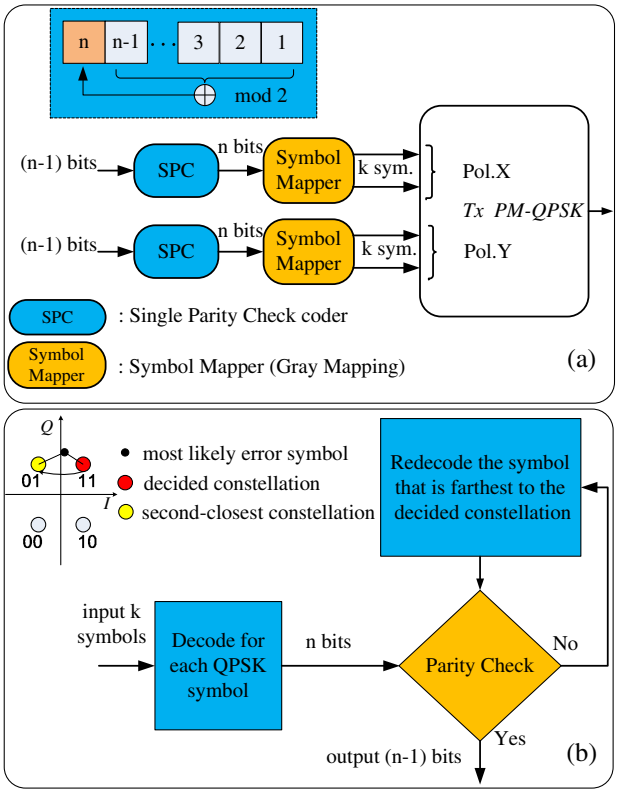

Fig. 1. (a) PM-kSC-QPSK implementation using the PM-QPSK hardware configuration and (b) joint-decision algorithm.

At the transmitter, the input bit stream of each polarization is divided into groups ($n-1$ bits for each group), and then the parity bit for each group is generated by the SPC coder. These n bits of each group are mapped into k consecutive QPSK symbols ($n=2k$ for QPSK), and the parity bit is inserted into the kth symbol. With the parity check bit, the kth QPSK symbol is limited to two kinds of phase states. At the receiver, most parts of the digital signal processing (DSP) algorithms of the standard PM-QPSK systems can be used for PM-kSC-QPSK, except for the decision algorithm. To make use of the parity check bit, we propose a joint-decision algorithm for k consecutive received symbols in each group. As shown in Fig. 1(b), first decode the input k symbols to get n bits ($n=2k$ for QPSK), then make the parity check for these n bits. If the parity is matching, output the front $n-1$ bits as the final decision results; else find the most likely error symbol from the input k symbols (we consider the received symbol that is farthest to the decided constellation as the most likely error symbol), and change its decision to the second closest constellation. Then the parity must be matching since the mapping rule is Gray mapping (only one bit difference for adjacent constellation).

To compare the PM-kSC-QPSK formats to the PM-QPSK formats, we use the SE[15]. The SE is defined as

$$\mathrm{SE}=\frac{\log_2 M}{N/2}, \tag{1}$$

where M is the number of constellation points, N is the number of dimensions, and $N=2k$ for coherent PM-kSC-QPSK. As a reference, we note that PM-QPSK has an SE of 2 bit/symbol/polarization. For the PM-kSC-QPSK formats $M=2^{2k-1}$. It can be shown that the SE for the PM-kSC-QPSK formats can be expressed as

$$\mathrm{SE}_{\text{PM-kSC-QPSK}}=2-\frac{1}{k}=\mathrm{SE}_{\text{PM-QPSK}}\left(1-\frac{1}{2k}\right). \tag{2}$$

When $k=2$, we get 4D modulation format PM-2SC-QPSK, which has the SE of 1.5 bit/symbol/polarization. When $k=4$, we get 8-dimensional modulation format PM-4SC-QPSK, which has a higher SE of 1.75 bit/symbol/polarization. The SE can be easily adjusted by using different values of k (every k consecutive symbols will be related).

Figure 2 shows the schematic of the experimental setup for the generation and detection of PM-2SC-QPSK and PM-4SC-QPSK at the symbol rates of 32 Gbaud (i.e., at the bit rates of 96 Gb/s for PM-2SC-QPSK and 112 Gb/s for PM-4SC-QPSK). At the transmitter, the parity bit for each group of $n-1$ bits is generated by the SPC coder, and then these n bits are mapped into k consecutive QPSK symbols, as shown in Fig. 2(a). The pseudo random binary sequence with a length of $2^{15}-1$ is used as the data bit sequence. The four field components of the encoded PM-2SC-QPSK or PM-4SC-QPSK signals, corresponding to the in-phase and quadrature (I/Q) components of both x and y polarizations, are

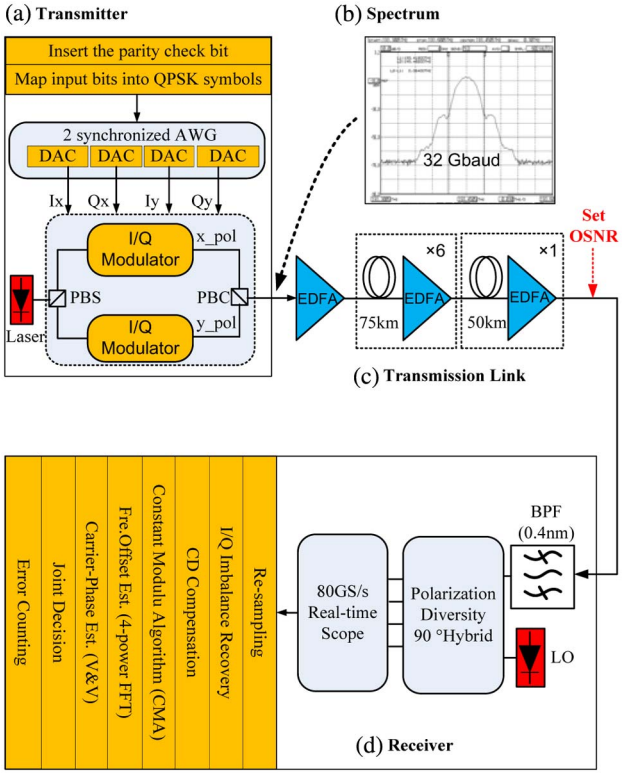

Fig. 2. Experimental setup for the 500 km PM-kSC-QPSK transmission system at 32 Gbaud. (a) Transmitter, (b) spectrum of the modulated signal, (c) transmission link, and (d) receiver.

entered in four 64 GSample/s digital-to-analog converters (DACs). Twofold oversampling is used, leading to a symbol rate of 32 Gbaud. The DAC outputs are amplified before driving a PM-I/Q modulator. The optical carrier is from an external cavity laser (ECL) at 193.475 THz with a linewidth of ~100 kHz. It should be noted that we can also use this experimental setup for a standard PM-QPSK except for the DSP of the transmitter and receiver.

The transmission link consists of six 75 km spans and one 50 km span of standard single-mode fiber, followed by an erbium-doped fiber amplifier (EDFA) with a 7 dB noise figure in each span to compensate for the fiber loss. OSNR can be adjusted by changing the noise figure of the EDFA at the front end of the receiver. Before the coherent receiver, the signal is amplified and filtered (0.4 nm), as shown in Fig. 2(b).

The front end of the coherent receiver consists of a polarization diverse 90° optical hybrid with integrated balanced detectors and the electrical signals are sampled at 80 GSample/s by the Lecroy WaveMaster-8-Zi and transferred to a computer for offline processing, as shown in Fig. 2(d). Then the signal is re-sampled to 2 samples per symbol, followed by I/Q imbalance and chromatic dispersion (CD) compensation. Since the polarization tributaries are independent for PM-kSC-QPSK, it can be easily polarization demultiplexed by the conventional constant modulus algorithm (CMA), while it does not work for PS-QPSK[16]. The linewidth of the local oscillator ECL is ~100 kHz. We use fast Fourier transform (FFT)-based compensation[17] for its frequency offset with respect to the signal laser (it is <100 MHz in the experiment) and perform phase estimation with the block-based Viterbi–Viterbi algorithm[18] (using blocks of 32–64 samples). Then, the decisions for each group of k symbols are obtained by using the joint-decision algorithm we proposed.

Figure 3(a) shows the B2B performance as a function of the OSNR for PM-2SC-QPSK and PM-4SC-QPSK compared to PM-QPSK at 32 Gbaud (i.e., at the bit rates of 96 Gb/s for PM-2SC-QPSK, 112 Gb/s for PM-4SC-QPSK, and 128 Gb/s for PM-QPSK). PM-2SC-QPSK requires 2.4 dB less OSNR to achieve a BER of 10^{-3} than for PM-QPSK, which is similar to PS-QPSK[19], and both PM-2SC-QPSK and PS-QPSK sacrifice 25% SE compared to PM-QPSK. PM-4SC-QPSK requires 1.7 dB less OSNR to achieve a BER of 10^{-3} than for PM-QPSK, at the expense of 12.5% SE reduction. The PM-4SC-QPSK has a performance compromise between the PM-2SC-QPSK and PM-QPSK. Figure 3(b) shows the measured B2B constellations at 15.7 dB OSNR (the same for PM-2SC-QPSK, PM-4SC-QPSK, and PM-QPSK). Figure 3(c) shows the BER performance after 500 km transmission. At a BER $= 10^{-3}$, the transmission penalty is only 0.1 dB for PM-2SC-QPSK, 0.4 dB for PM-4SC-QPSK, and 0.7 dB for PM-QPSK so that there are 3 and 2 dB improvement, respectively, for PM-2SC-QPSK and PM-4SC-QPSK, compared to PM-QPSK at 32 Gbaud.

To improve the SE further, we will apply the flexible multidimensional modulation method to higher-order modulation formats (such as PM-16QAM) in our future work.

As a summary of the experimental results, Table 1 shows a comparison of the flexible multidimensional modulation formats for the achievable SE and the Rx sensitivity.

It can be seen that by adjusting the number of related symbols, the SE and Rx sensitivity can be easily adjusted for different network transmission paths. For these multidimensional modulation formats, the hardware configuration and main DSP algorithms are compatible with the PM-QPSK format. Hence, it is more effective than using the adaptive FEC codes, which requires significant

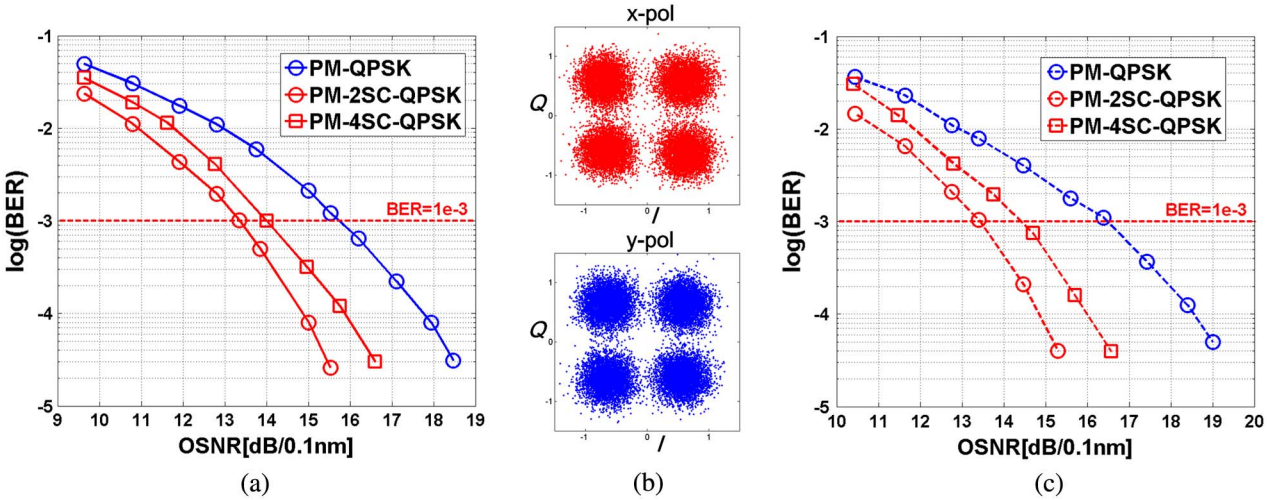

Fig. 3. (a) Measured B2B BER for PM-2SC-QPSK, PM-4SC-QPSK, and PM-QPSK at 32 Gbaud (i.e., at the bit rates of 96 Gb/s for PM-2SC-QPSK, 112 Gb/s for PM-4SC-QPSK, and 128 Gb/s for PM-QPSK). (b) Constellations measured back to back at 15.7 dB OSNR. (c) The measured BER after 500 km transmission for PM-QPSK, PM-2SC-QPSK, and PM-4SC-QPSK at 32 Gbaud.

Table 1. Multidimensional Modulation Formats and Their Characteristics

Formats	SE (bit/sym/pol)	Info/Gross Bit rate (Gb/s)	Rx Sensitivity[a] (dB/0.1 nm)
PM-QPSK	2	128/128	15.7
PM-2SC-QPSK	1.5	96/128	13.3
PM-4SC-QPSK	1.75	112/128	14

[a]Back to back Rx sensitivity at BER $= 10^{-3}$.

additional hardware effort to get the system flexibility. This flexible multidimensional modulation methods can be applied to the transceivers of elastic optical networks to support the fine-granularity adjustment in the trade-off among bit rate, SE, and OSNR tolerance.

This work was supported by the National Natural Science Foundation of China (No. 61571061) and the Fund of State Key Laboratory of Information Photonics and Optical Communications (Beijing University of Posts and Telecommunications), China.

References

1. O. Gerstel, M. Jinno, A. Lord, and S. J. B. Yoo, IEEE Comm. Magazine **50**, s12 (2012).
2. S. Gringeri, N. Bitar, and T. J. Xia, IEEE Comm. Magazine **51**, 32 (2013).
3. K. Roberts and C. Laperle, in *European Conference on Optical Communication (ECOC)*, We.3.A.3 (2012).
4. G. Bosco, V. Curri, A. Carena, P. Poggiolini, and F. Forghieri, J. Lightwave Technol. **29**, 53 (2011).
5. Y. Sun, L. Xi, X. Tang, D. Zhao, Y. Qiao, X. Zhang, and X. Zhang, Chin. Opt. Lett. **12**, 100606 (2014).
6. C. Li, M. Luo, X. Xiao, J. Li, Z. He, Q. Yang, Z. Yang, and S. Yu, Chin. Opt. Lett. **12**, 040601 (2014).
7. J. Xiao, C. Tang, X. Li, J. Yu, X. Huang, C. Yang, and N. Chi, Chin. Opt. Lett. **12**, 050603 (2014).
8. X. Zhou, L. E. Nelson, and P. Magill, IEEE Comm. Mag. **51**, 41 (2013).
9. G.-H. Gho and J. M. Kahn, J. Lightwave Technol. **30**, 1818 (2012).
10. M. Karlsson and E. Agrell, Opt. Express **17**, 10814 (2009).
11. G. Ungerboeck, IEEE Trans. Inf. Theory **28**, 55 (1982).
12. J. Renaudier, P. Serena, A. Bononi, M. Salsi, O. Bertran-Pardo, H. Mardoyan, P. Tran, E. Dutisseuil, G. Charlet, and S. Bigo, J. Lightwave Technol. **30**, 1312 (2012).
13. M. Sjödin, P. Johannisson, H. Wymeersch, P. A. Andrekson, and M. Karlsson, Opt. Express **19**, 7839 (2011).
14. M. Sjödin, P. Johannisson, J. Li, E. Agrell, P. A. Andrekson, and M. Karlsson, Opt. Express **20**, 8356 (2012).
15. E. Agrell and M. Karlsson, J. Lightwave Technol. **27**, 5115 (2009).
16. P. Johannisson, M. Sjödin, M. Karlsson, H. Wymeersch, E. Agrell, and P. A. Andrekson, Opt. Express **19**, 7734 (2011).
17. M. Selmi, Y. Jaouën, and P. Ciblat, in *Proceedings of ECOC*, P3.08 (2009).
18. A. J. Viterbi and A. M. Viterbi, IEEE Trans. Inf. Theory **29**, 543 (1983).
19. M. Sjödin, P. Johannisson, H. Wymeersch, P. A. Andrekson, and M. Karlsson, Opt. Express **19**, 7839 (2011).